

Supporting Information for:

Metal ion directed metal-organic rotaxane frameworks with intrinsic features of self-penetration and interpenetration

Jun Liang,^a Xin-long Wang,^{*a} Yan-Qing Jiao,^a Chao Qin,^a Kui-Zhan Shao,^a Zhong-Min Su^{*a} and Qing-Yin Wu^b

^aInstitute of Functional Material Chemistry, Key Lab of Polyoxometalate Science of Ministry of Education, Faculty of Chemistry, Northeast Normal University, Changchun, 130024 Jilin, People's Republic of China.

^bDepartment of Chemistry, Zhejiang University

Table of Contents	Page
General Comments	S-3
X-ray Structure determination	S-3
Details for Electrochemical Experiments.	S-4
Scheme S1 for MORFs 1(Cu), 2 (Zn) and 3(Cd).	S-5
Synthesis of [C6CN4 ²⁺] \cdot 2[NO ₃] ⁻ .	S-5
Synthesis of [PCN64 ²⁺] \cdot 2[NO ₃] ⁻ .	S-5
Fig. S1. ¹ H NMR spectrum of [C6CN4 ²⁺] \cdot 2[NO ₃] ⁻ (500 MHz in D ₂ O).	S-6
Fig. S2. ¹ H NMR spectrum of [PCN64 ²⁺] \cdot 2[NO ₃] ⁻ (500 MHz in D ₂ O).	S-6
Preparation of 1 [Cu(PCA64)(PCA64 ²⁻)] \cdot 13H ₂ O.	S-7
Preparation of 2 and 3.	S-7
Fig. S3. Powder-XRD results for compounds 1, 2 and 3.	S-7
Fig. S4. The IR spectrum of compounds 1, 2 and 3.	S-8
Fig. S5. The single three-dimensional mok structure of 1 without CB6.	S-8
Fig. S6. The 3-fold interpenetration of mok frameworks in 1.	S-8
Fig. S7. Thermal gravimetric analysis (TGA) curve for as-synthesized 1.	S-9
Fig. S8. The 2-fold helical chains in 1.	S-9
Fig. S9. Emission spectra of compounds 1, 2, 3 and PCA64.	S-10
Fig. S10. Schematic view of the closest four CB[6]s around each Cu center.	S-10
Fig. S11. The different outer-rotaxanic hydrogen bonding styles of PCA64	S-11
Fig. S12. Single crystal X-ray structure of PCN64 and PCA64.	S-11

Fig.S13. Variable temperature PXRD data for **1**. S-12

Fig. S14. The PXRD data (blue) of **1** after immersion in 1 M NaCl+H₂SO₄ (pH=1) for 30 minutes and the simulated **1** (black). S-12

Fig. S15. The cyclic voltammograms of the **1-CPE** in 1 M NaCl+H₂SO₄ (pH=1). S-12

General Comments

CB[6] was synthesized according to references¹. Other reagents were purchased from commercial sources and used as received. The Fourier transform infrared (FT-IR) spectra were recorded from KBr pellets in the range of 4000–400 cm⁻¹ on a Mattson Alpha-Centauri spectrometer. Elemental analyses (C, H, and N) were performed on a Perkin-Elmer 2400 elemental analyzer. Cu was determined with a Plasma-SPEC(I) ICP atomic emission spectrometer. ¹H NMR solution experiments were performed on a Bruker Avance 500 instrument, with working frequencies of 499.8 MHz for ¹H nuclei. Chemical shifts are quoted in ppm relative to tetramethylsilane using the residual solvent peak as a reference standard. Thermogravimetric analysis (TGA) was performed on a Perkin-Elmer TG-7 analyzer over the temperature 40–800 °C in a nitrogen-gas atmosphere with a heating rate of 10 °C min⁻¹. Solid-state luminescent spectra were measured on a Cary Eclipse spectrofluorometer (Varian) equipped with a xenon lamp and quartz carrier at room temperature. Powder XRD measurements were recorded on a Siemens D5005 diffractometer with Cu K α (λ = 1.5418 Å) radiation in the range 5–50°.

1. (a) Day, A.; Arnold, A. P.; Blanch, R. J. and Snushall, B. J. *Org. Chem.*, **2001**, 66, 8094–8100; (b) Kim, J.; Jung, In-S.; Kim, S. Y.; Lee, E.; Kang, J. K.; Sakamoto, S.; Yamaguchi, K. and Kim, K. J. *Am. Chem. Soc.*, **2000**, 122, 540–541.

X-ray Structure determination

X-ray diffraction data collection of the compounds was performed on a Bruker Smart Apex II CCD diffractometer with graphite-monochromated Mo-K α radiation (λ = 0.71073 Å) at room temperature. All absorption corrections were performed by using the SADABS program. The crystal structure was solved by the Direct Method of SHELXS-97 and refined with full-matrix least-squares techniques (SHELXL-97) within WINGX. **PCN64**: C₅₈H₇₈N₂₈O₁₉, *Mr* = 1471.8, Monoclinic, *C*2/*c*, *a* = 28.266(5) Å, *b* = 15.802(5) Å, *c* = 18.367(5) Å, β = 119.599(5)°, *V* = 7133(3) Å³, *Z* = 4, $\rho_{\text{calcd.}}$ = 1.370 Mg m⁻³, final *R*₁ = 0.1312 and *wR*₂ = 0.3800 (*R*_{int} = 0.0436) for 17970 independent reflections [*I* > 2 σ (*I*)]. **PCA64**: C₅₈H₈₁N₂₆O_{23.5}, *Mr* = 1518.49, Triclinic, *P*-1, *a* = 12.485(5) Å, *b* = 17.202(5) Å, *c* = 17.659(5) Å, α = 94.549(5)°, β = 93.303(5)°, γ = 111.017(5)°, *V* = 3514(2) Å³, *Z* = 2, $\rho_{\text{calcd.}}$ = 1.435 Mg m⁻³, final *R*₁ = 0.1483 and *wR*₂ = 0.4220 (*R*_{int} = 0.0640) for 18336 independent reflections [*I* > 2 σ (*I*)]. **1 [Cu(PCA64)(PCA64²⁻)]·13H₂O**: CuC₁₁₆H₁₅₀N₅₂O₄₅, *Mr* = 3056.42, Monoclinic, *C*2/*c*, *a* = 37.209(5) Å, *b* = 37.083(14) Å, *c* = 23.517(7) Å, β = 113.162(5)°, *V* = 29834(9) Å³, *Z* = 8, $\rho_{\text{calcd.}}$ = 1.361 Mg m⁻³, final *R*₁ = 0.1347 and *wR*₂ = 0.4439 (*R*_{int} = 0.1009) for 77397 independent reflections [*I* > 2 σ (*I*)]. **2 [Zn(PCA64)(PCA64²⁻)]·13H₂O**: ZnC₁₁₆H₁₄₆N₅₂O₄₃, Monoclinic, *a* = 37.93 Å, *b* = 37.93 Å, *c* = 23.61 Å, β = 113.78°, *V* = 31087 Å³. **3 [Cd(PCA64)(PCA64²⁻)]·13H₂O**: CdC₁₁₆H₁₄₆N₅₂O₄₃, Monoclinic, *a* = 37.614 Å, *b* = 37.630 Å, *c* = 23.41 Å, β = 113.71°, *V* = 30338 Å³. The crystal data of compounds **2** and **3** are not good enough to obtain the crystal structures. We have only get the cell parameters and they are very close to the compound **1**. Furthermore, The PXRD confirm that the compound **1**, **2** and **3** are isostructures. CCDC 938011 (**PCN64**), 938012 (**PCA64**) and 938013 (**1**) contain the supplementary crystallographic data for this paper. These data

can be obtained free of charge from the Cambridge Crystallographic Data Centre via www.ccdc.cam.ac.uk/data_request/cif for **1**, **PCN64** and **PCA64**.

Details for Electrochemical Experiments

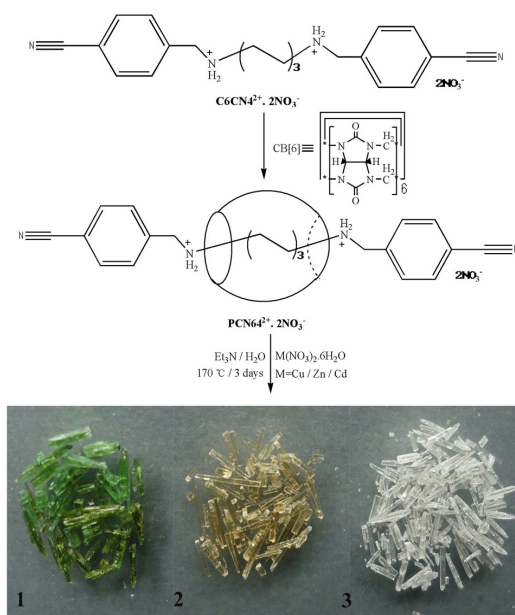
Materials. High purity graphite powder (average particle 1-2 μm) was obtained from Aldrich. Paraffin oil was purchased from Beijing Chemical Plant and used as received. Other chemicals were of analytical grade and used without further purification.

Apparatus. A CHI 660 Electrochemical Workstation connected to a Digital-586 personal computer was used for control of the electrochemical measurements and for data collection. A conventional three-electrode cell, consisting a 1-modified carbon paste electrode or a glassy carbon electrode as the working electrode, a saturated silver reference electrode and a Pt wire counter electrode was used. All potentials were measured and reported versus the Ag^+/Ag . All the experiments were conducted at room temperature (25-30°C).

Preparation of carbon paste electrode modified by compound 1 (1-CPE)

Compound **1** modified CPE (**1-CPE**) was fabricated by the following process: 0.33g graphite powder was added to the solution of 8 mL ethanol containing 30mg **1** and the mixture was ultrasonically mixed for 10 min, followed by evaporation of ethanol under vacuum, which produced rather homogenously covered graphite particles. To the graphite 0.2 mL paraffin oil was added and stirred with a glass rod; then the mixture was prepared to pack into 3 mm inner diameter glass tube to a length of 0.8 cm from one of its end, and the surface was pressed tightly on smooth plastic paper with a copper rod through the back. Electrical contact was established with a copper rod through the back of the electrode.

Synthesis



Scheme S1. Synthetic steps involved in the preparation of MORFs **1** (Cu), **2** (Zn) and **3** (Cd). The barrel-like cartoon is a simplified depiction of CB[6].

[C6CN4²⁺]·2[NO₃]⁻: A solution of 4-cyanobenzaldehyde (2.00 g, 15.24 mmol) in MeOH (100 mL) was added to a solution of 1,6 -diaminobutane (0.844g, 7.26 mmol) in MeOH (50 mL) and the mixture was heated at reflux for 20 h. When the solution was cooled down to room temperature, NaBH₄ (1.00 g, 26.4 mmol) was added little by little before the mixture was refluxed for another 12 h. The solvent was removed in vacuo and the white residue was dissolved in a small amount of distilled water. After the aqueous solution was basified with NaOH(s) (pH>12), the product was extracted with dichloromethane. The extract was dried over magnesium sulfate and evaporated in vacuo. The white solid was dissolved in 300ml EtOH and excess amount of HNO₃ was added to the solution to precipitate the product, which was then filtered, washed with EtOH and dried in vacuo (2.71g, 80%). Mp >212°C (decomp); ¹H NMR (500MHz, D₂O): δ= 1.14 (s, 4H), 1.46 (s, 4H), 2.84 (br, 4H), 4.07 (s, 4H), 7.38 (d, 4H), 7.62 (d, 4H); Anal. Calcd(Found%) for C₂₂H₂₈N₆O₆·2H₂O: C, 51.97 (51.10); N, 16.53 (16.42); H, 6.30 (6.43).

[PCN64²⁺]·2[NO₃]⁻: To a solution of [C6CN4²⁺]⁺·2[NO₃]⁻ (1.066 g, 2.26 mmol) in water (300 mL) was added CB[6] (3.06 g, 2.6 mmol). Then the mixture was put in an ultrasonic instrument for 30 mins before heating at reflux for 3 h. After that, undissolved CB[6] was filtered off. When the volume of the filtrate was reduced to ~80 mL, heating was stopped. After several hours, considerable amount of colorless crystals came out. Ethanol (300 mL) was added to the solution to precipitate more product, which was filtered, washed with EtOH and dried in vacuo (2.67g, 70%). Mp >324°C (decomp); ¹H NMR (500MHz, D₂O): δ= 0.26 (s, 4H), 0.63 (s, 4H), 2.82 (s, 4H), 4.22 (s, 4H), 4.08 (d, 12H), 5.34 (s, 12H), 5.47(d, 12H), 7.64 (s, 8H). IR (cm⁻¹): ν(C-H) 3072, 2928; ν(C≡N) 2231; ν(C=O) 1739; ν(CH₂) 1473.

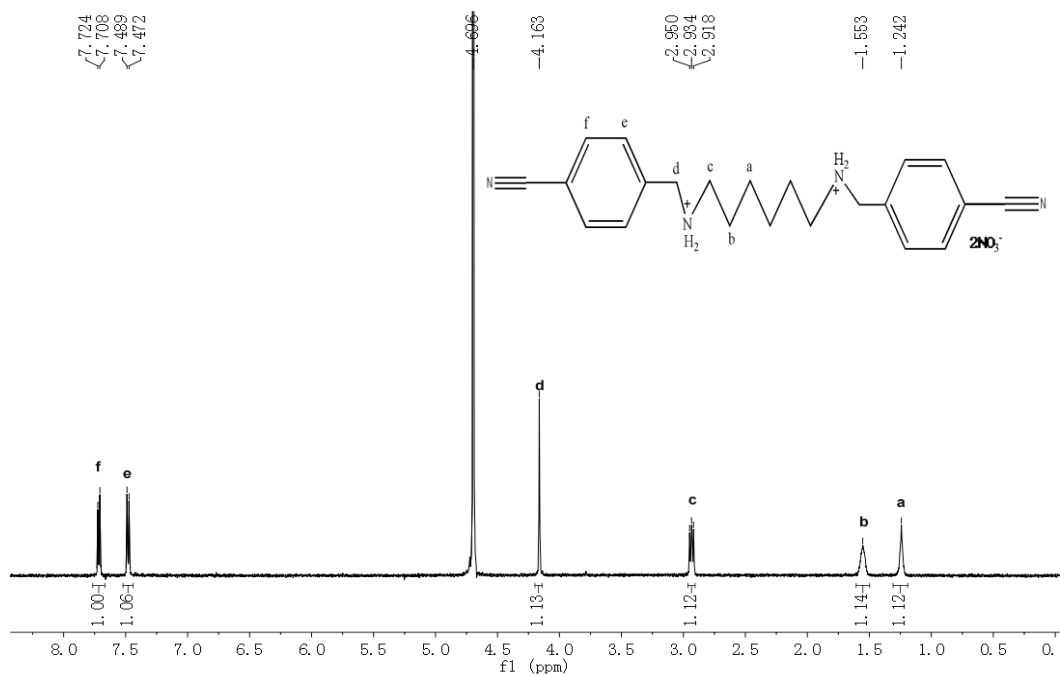


Fig. S1. ¹H NMR spectrum of [C6CN4²⁺]·2[NO₃⁻] (500 MHz in D₂O).

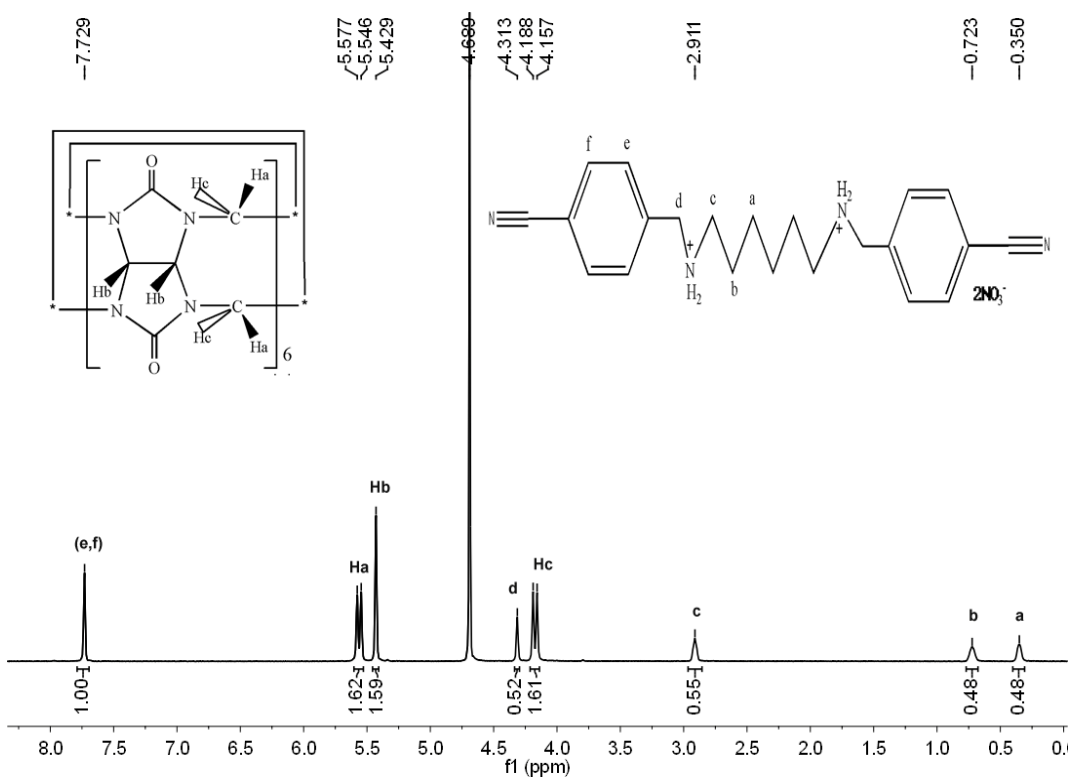


Fig. S2. ¹H NMR spectrum of [PCN64²⁺]·2[NO₃⁻] (500 MHz in D₂O).

Preparation of **1** [Cu(PCA64)(PCA64²⁻)]·13H₂O

[PCN64²⁺]⁺·2[NO₃]⁻ (0.168 g, 0.1 mmol), Cu(NO₃)₂·3H₂O (45 mg, 0.19 mmol), triethylamine (3 drops, where 1 ml injection syringe is used) were suspended in water (6 ml) in a stainless-steel bomb, which was then sealed, kept at 170°C for 72 h, and cooled to room temperature at a constant cooling rate of 10°C h⁻¹. Large, green crystals of **1** were washed with water several times, collected by manual operation and dried in air (92 mg, 60%). IR (cm⁻¹): ν(C-H) 3000, 2935; ν(C=O) 1736; ν(CH₂) 1474. Anal. Calcd(Found%): Cu, 2.07 (1.98); C, 45.78 (44.96); N, 23.81 (23.63); H, 4.97 (4.52).

Preparation of **2** and **3**

Reaction of [PCN64²⁺]⁺·2[NO₃]⁻ with M(NO₃)₂·6H₂O (M=Zn, Cd) under similar conditions used to prepare compound **1** lead to two isomorphous MORFs, compound **2** (Zn) and **3** (Cd) as exhibited by the PXRD patterns shown in Figure. S3.

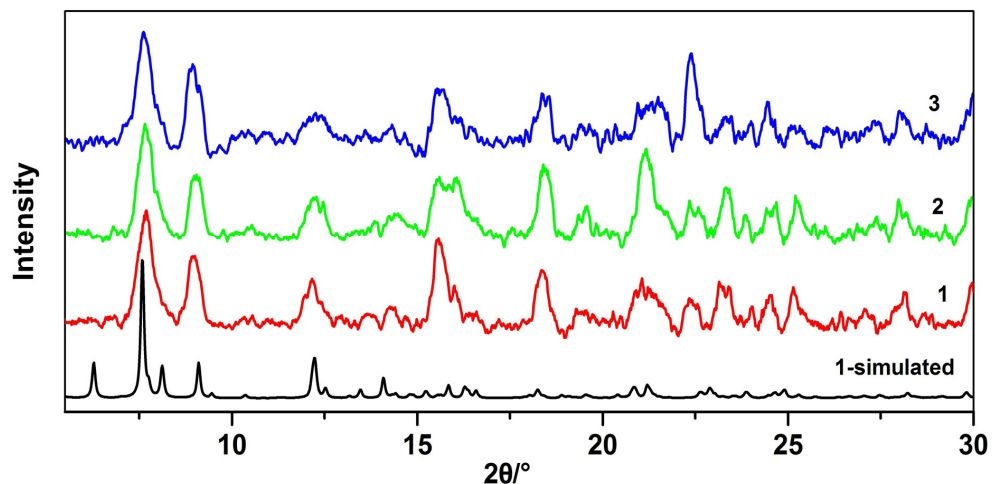


Fig. S3. Powder-XRD results for compound **1**, **2** and **3**. **Black** (simulated spectra from single crystal data of **1**). Products **1** to **3** give rise to similar PXRD spectra, leading us to suggest that these materials have analogous, if not identical structures.

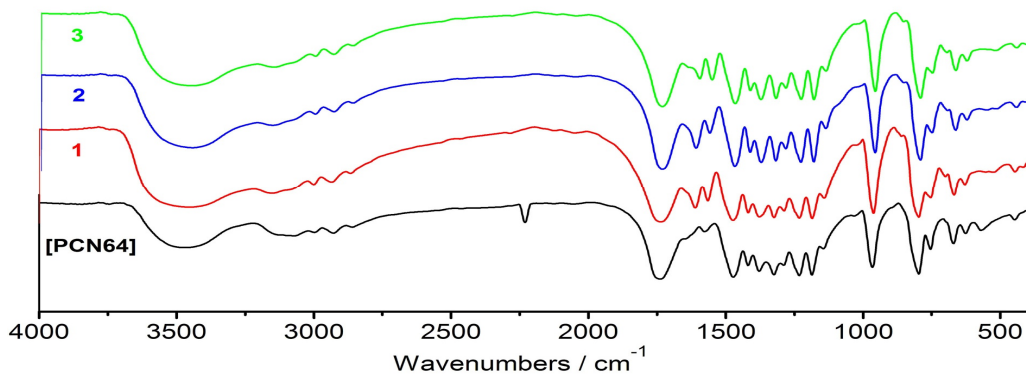


Fig. S4. The IR spectrum of compounds **1**, **2**, **3** and **L**([PCN64²⁺] \cdot 2[NO₃]). The IR spectrum of **L** exhibits a band at 2231 cm⁻¹ attributed to ν(C≡N).

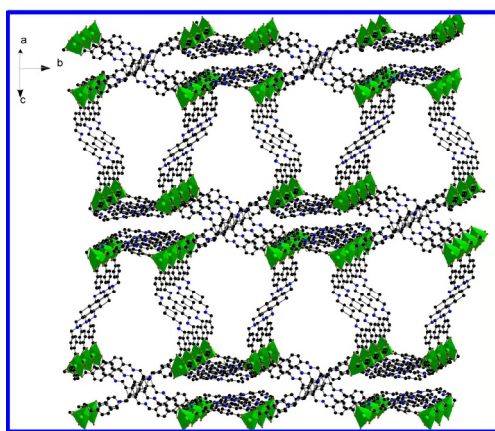


Fig. S5. Ball-and-stick representation of the single three-dimensional **mok** structure of **1** without CB6. Atom color code: C black, N blue, O red, Cu or polyhedra green.

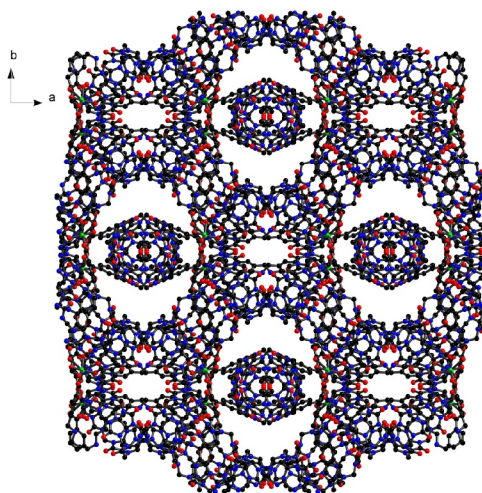


Fig. S6. Ball-and-stick representation of 3-fold interpenetration of **mok** framework as in **1**, showing the channels that contain the solvated water molecules.

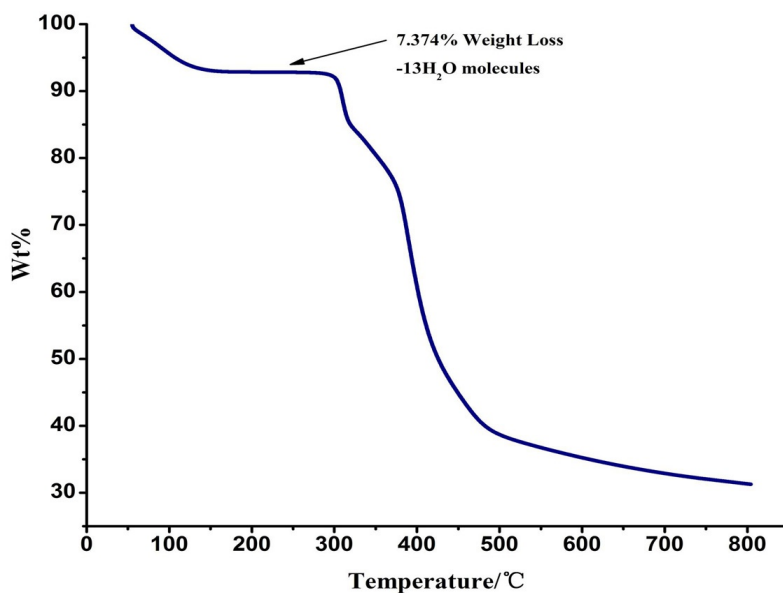


Fig. S7. Thermal gravimetric analysis (TGA) curve for as-synthesized **1**. Water of crystallization is volatilized from room temperature to about 170°C and organic ligand decomposed rapidly only after 300°C.

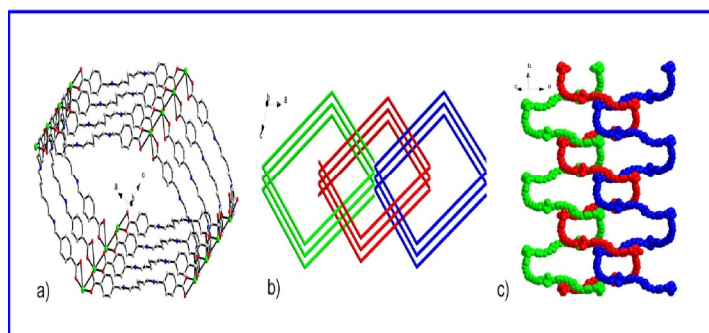


Fig. S8. a) The assembly of $\text{Cu}(\text{NO}_3)$ and $\text{PCA64}/\text{PCA64}^{2-}$ has also produced helical chains, in which *trans*-PCA64, Cu^{2+} and *cis*-PCA64²⁻ alternate, with a helical pitch of 37.08 and width of 37.06 Å. b) The entanglement of the nanotubes. c) Each helix is interwoven with other two belonging to different parallel nanotubes in **1**. CB6 is omitted for clarity.

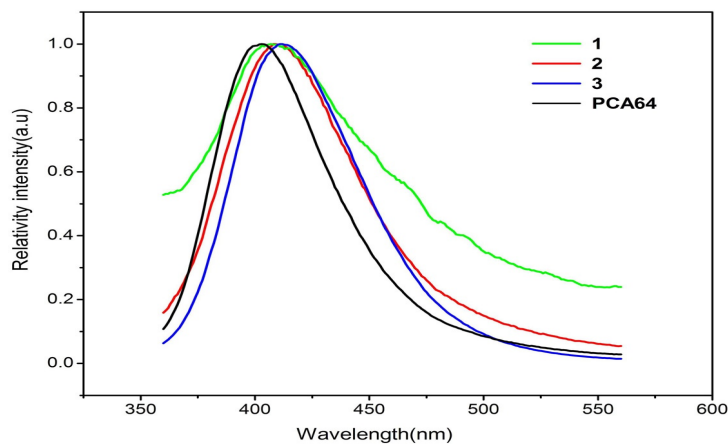


Fig. S9. Emission spectra of compounds **1**, **2**, **3** and **PCA64** in the solid state at room temperature, which illustrated that only intraligand (π - π^*) fluorescent emission occurred because all emissions were quite similar compared to that of PCA64 at 403 nm ($\lambda_{\text{ex}}=309\text{nm}$).

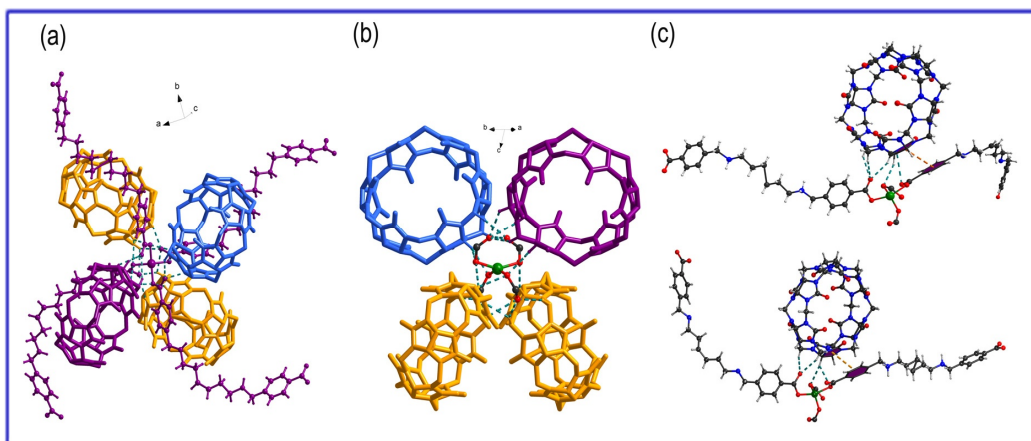


Fig. S10. a) Schematic view of the closest four CB[6]s belonging to three different networks (colored in violet, light blue and light orange, respectively) around each Cu center. b) Representation of the outer-rotaxanic hydrogen bonds ($\text{H}\cdots\text{O}$ distances ranges from 2.39 to 2.59 Å) between CB[6]s and c) carboxylic groups and π - π stacking interactions (average distance 3.466(8) Å) around each Cu center. Note: some hydrogen atoms are omitted for clarity. Dashed cyan and orange lines represent hydrogen bonding and π - π interactions, respectively.

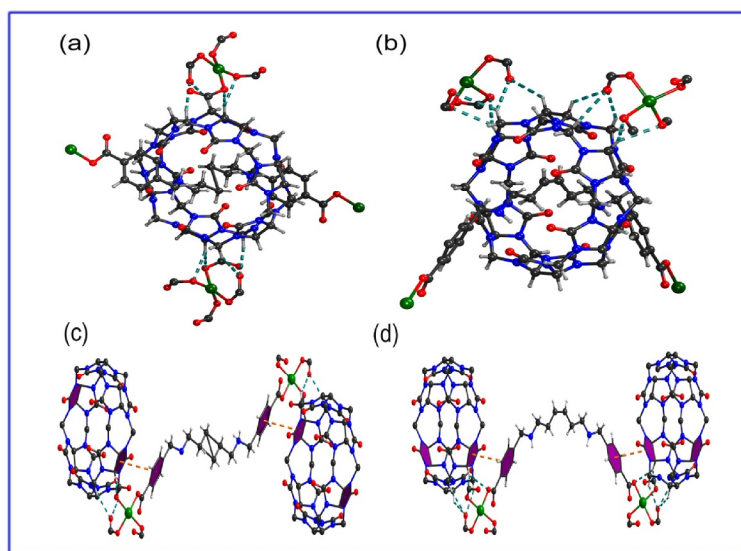


Fig. S11. The different outer-rotaxanic hydrogen bonding styles and π — π stacking interactions of *trans*-PCA64 (a, c) and *cis*-PCA64²⁻ (b, d) in **1**. Dashed cyan and orange lines represent hydrogen bonding and π — π interactions, respectively.

Single Crystal X-ray Structure of PCN64 and PCA64

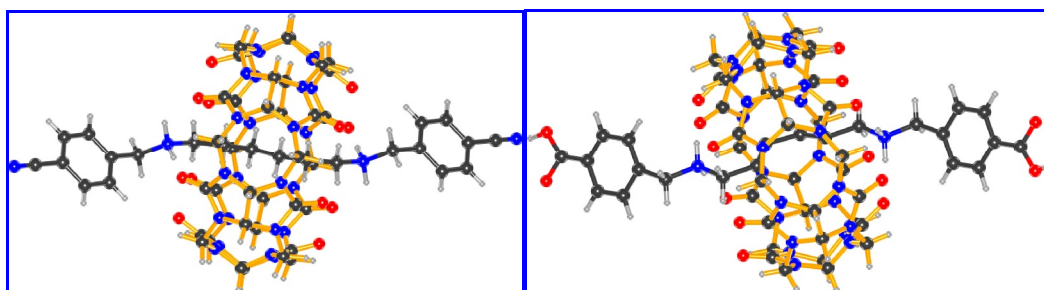


Fig. S12. A ball-and-stick representation of the X-ray structure of **PCN64** and **PCA64** with labeling scheme. Black, carbon; Blue, nitrogen; red, oxygen; gray, hydrogen.

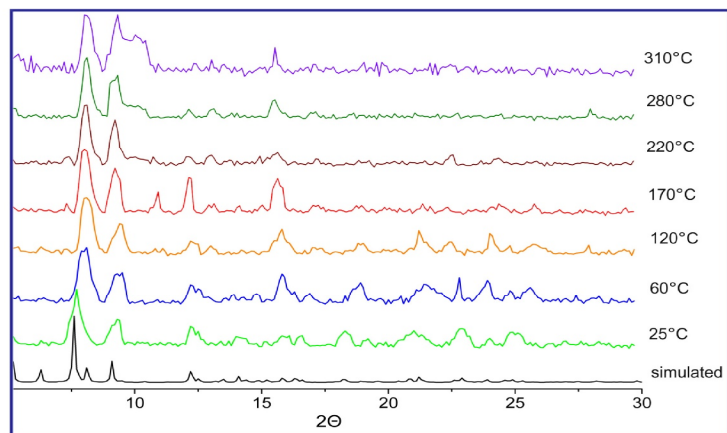


Fig. S13. Variable temperature PXRD data for **1**.

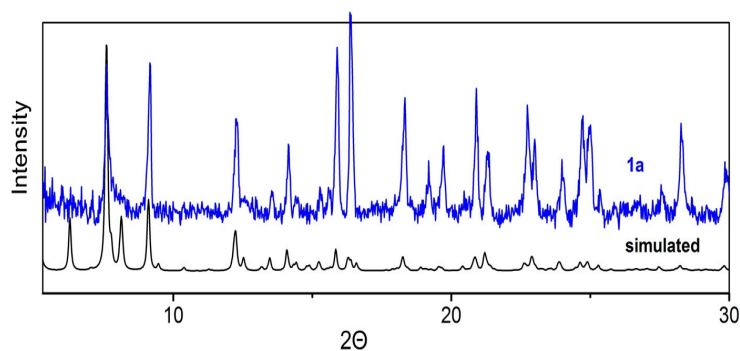


Fig. S14. The PXRD data (blue) of **1** after immersion in 1 M NaCl+H₂SO₄ (pH=1) for 30 minutes and the simulated **1** (black).

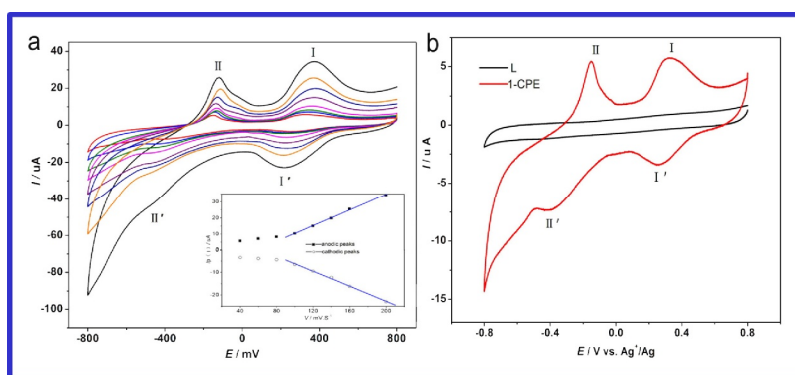


Fig. S15 (a) The cyclic voltammograms of the **1-CPE** in 1 M NaCl+H₂SO₄ (pH=1) at different scan rates (from inner to outer: 40, 60, 80, 100, 120, 140, 160, and 200 mV·s⁻¹). (b) Comparisons of the voltammetric behaviors of **1-CPE** and **L** ([PCN64] in H₂SO₄ (pH=1); scan rate: 40 mV·s⁻¹; working electrode: glassy carbon (3 mm). The inset shows the anodic peak (I) and cathodic peak (I') currents are proportional to the scan rates higher than 100 mV·s⁻¹.